Overlapping Effects of S3 Stalk Segment Mutations on the Affinity of Ca^{2+}-ATPase (SERCA) for Thapsigargin and Cyclopiazonic Acid†

Hailun Ma, Lilin Zhong, and Giuseppe Inesi

Department of Biochemistry and Molecular Biology, University of Maryland School of Medicine, Baltimore, Maryland 21201

Isabel Fortea, Fernando Soler, and Francisco Fernandez-Belda*

Departamento de Bioquimica y Biologia Molecular A, Veterinaria, Universidad de Murcia, Espinardo, 30071 Murcia, Spain

Received July 1, 1999; Revised Manuscript Received September 14, 1999

ABSTRACT: Chimeric exchanges and mutations were produced in the Ca^{2+}-ATPase (SERCA) to match (in the majority of cases) corresponding sequences of the Na^+,K^+-ATPase. The effects of these mutations on the concentration dependence of the specific Ca^{2+}-ATPase inhibition by thapsigargin (TG) and cyclopiazonic acid (CPA) were then determined. Extensive chimeric mutations on the large cytosolic loop, on the S4 stalk segment, and on the M3 transmembrane segments produced little or no modification of the Ca^{2+}-ATPase sensitivity to either inhibitor. On the other hand, the presence of a six amino acid Na^+,K^+-ATPase sequence within the S3 stalk segment of the Ca^{2+}-ATPase raised 60-fold the apparent K_i for TG and 250-fold the apparent K_i for CPA. More limited mutations within the same S3 segment, however, affected differently the concentration dependence of the Ca^{2+}-ATPase inhibition by TG or CPA. Specifically, single mutation of Phe256 to Val increased 20-fold the apparent K_i for TG, while having very little effect on the apparent K_i for CPA. These findings indicate significant overlap of the TG and CPA binding domains within the S3 stalk segment of the Ca^{2+}-ATPase, where the contribution of each protein residue is dependent on the structures of the two inhibitors. Saturating concentrations of either or both TG and CPA produce an identical reduction of the affinity of the ATPase for ATP, suggesting that only one inhibitor can bind at any time due to significant overlap of their binding domains. It is suggested that perturbations produced by binding of either inhibitor within the stalk segment interfere with the long-range functional linkage between ATP utilization in the ATPase cytosolic region and Ca^{2+} binding in the membrane-bound region.

Thapsigargin (TG[1]), a sesquiterpene lactone derived from the plant *Thapsia garganica* (*1*), and cyclopiazonic acid (CPA), a secondary metabolite of certain *Penicillum* and *Aspergillus* fungi (*2*), are specific and potent inhibitors of sarco-endoplasmic reticulum Ca^{2+}-ATPases (SERCA) (*3*−*7*). Previous mutational studies of the Ca^{2+}-ATPase (here after used to indicate SERCA) showed that chimeric replacement of the entire transmembrane and stalk segment (M3−S3) of the Ca^{2+}-ATPase with the corresponding segment of the Na^+,K^+-ATPase reduces the sensitivity of the Ca^{2+}-ATPase to TG (*8*−*10*). It was then found (*11*) that it is actually the S3 stalk segment that is specifically involved in determining the Ca^{2+}-ATPase affinity for TG. We report here a comparative mutational analysis of the concentration dependence of ATPase inhibition by TG and CPA, demonstrating that the S3 stalk segment has an influence on the ATPase affinity for both inhibitors. Mutations of specific amino acid within the same segment, however, affect differently the apparent affinity of the enzyme for TG or CPA. We also report experiments suggesting that occupancy of the same binding domain by either TG or CPA is involved in decreasing the Ca^{2+}-ATPase affinity for ATP.

MATERIALS AND METHODS

Recombinant DNA Constructs. The cDNA encoding the chicken fast muscle SERCA1a isoform of the Ca^{2+}-ATPase (*12*) was used for PCR mutagenesis by the overlap extension method (*13*). This method, as adapted by Zhong and Inesi (*11*), was used sequentially to produce additive mutations. On the other hand, the chicken Na^+,K^+-ATPase α1 subunit (*14*) was used for chimeric replacement of a large portion of the SERCA1 cytosolic loop (scheme A in Figure 1) as described by Sumbilla et al. (*8*).

The final constructs were subcloned in mammalian expression vector pcDL-SR α296 (*15*) for transfection of COS-1 cells by the DEAE-dextran method (*16*), as adapted by Sumbilla et al. (*8*). The cells were harvested 72 h after transfection.

Microsomal Preparation and Immunodetection of Ca^{2+}-ATPase Expression. The microsomal fraction of transfected

† This research was supported by the National Institutes of Health (PO1 HL27867), the Spanish Ministerio de Educacion y Cultura (PB97-1039), and the U.S.−Spain Joint Commission for Scientific and Technological Cooperation.

* Corresponding author. Telephone: +34 968 364 763. Fax: +34 968 364 147. E-mail:fbelda@fcu.um.es

[1] Abbreviations: CPA, cyclopiazonic acid; MOPS, 4-morpholinepropanesulfonic acid; M, transmembrane segment; S, stalk segment; SERCA, sarco-endoplasmic reticulum Ca^{2+}-ATPase; SR, sarcoplasmic reticulum; TG, thapsigargin; TNP-ATP, 2′,3′-*O*-(2,4,6-trinitrocyclohexadienylidene)-adenosine-5′-triphosphate; WT, wild type.

10.1021/bi991523q CCC: $18.00
Published on Web 11/06/1999

cells was obtained by differential centrifugation of disrupted cells as described by Strock et al. (*17*). Immunodetection of Ca^{2+}-ATPase expression was obtained by Western blotting, using the CaF-5C3 monoclonal antibody (*12*). Large chimeric replacement of the cytosolic region of the Ca^{2+}-ATPase with the corresponding region of the Na^+,K^+-ATPase was detected with a monoclonal antibody to the Na^+,K^+-ATPase α1 subunit (*18*).

Preparation of Sarcoplasmic Reticulum (SR) Vesicles from Skeletal Muscle. The microsomal fraction enriched in Ca^{2+}-ATPase protein (SR vesicles) was isolated from rabbit leg white muscle according to Eletr and Inesi (*19*).

Total protein concentration in COS-1 cell microsomes and SR vesicles was measured by the colorimetric procedure of Lowry et al. (*20*), standardized with bovine serum albumin.

ATPase activity was assayed in a reaction mixture containing 20 mM MOPS, pH 7.0, 80 mM KCl, 3 mM $MgCl_2$, 0.2 mM $CaCl_2$, 5 mM sodium azide, 20 μg of microsomal protein/mL, 3 μM ionophore A23187, 3 mM ATP, and 0−5 μM TG or 0−300 μM CPA. Ca^{2+}-independent ATPase activity was assayed in the presence of 2.0 mM EGTA and no added Ca^{2+}. The reaction was started (37 °C) by the addition of ATP, and samples were taken at serial times for determination of P_i by the method of Lanzetta et al. (*21*). The Ca^{2+}-dependent ATPase activity was estimated by subtracting the Ca^{2+}-independent ATPase from the total ATPase. The ATPase activity was also corrected to account for the level of expressed ATPase protein in each microsomal preparation, as revealed by immunoreactivity and with reference to a standard preparation of microsomes obtained from COS-1 cells transfected with WT SERCA1 cDNA.

Phosphorylated intermediate steady-state levels were determined by first adding the experimental concentration of TG or CPA (or an equal volume of solvent) to an ice-cold reaction mixture containing 20 mM MOPS, pH 7.0, 80 mM KCl, 5 mM $MgCl_2$, 1.0 mM EGTA, and 15−30 μg of microsomal protein. Following 10 min incubation, an equal volume of a mixture containing 20 mM MOPS, pH 7.0, 80 mM KCl, 5 mM $MgCl_2$, 1.0 mM $CaCl_2$, and 20 μM [γ-^{32}P]-ATP was added by rapid mixing. After 10 s incubation, the reaction was quenched with 0.4 mL of 4 M perchloric acid. The quenched samples were transferred onto Eppendorf tubes containing 100 μg of carrier protein and centrifuged at 5000*g* for 5−10 min. The sediment was washed twice with 0.125 M perchloric acid and once with cold distilled water. The entire procedure was carried out in the cold room. The samples were then solubilized and subjected to electrophoresis at pH 6.3 (*22*). The radioactive phosphoenzyme intermediate was then detected by autoradiography and phosphoimaging.

TNP-ATP binding to SR ATPase was assessed with the aid of a Bio-Logic (Claix, France) modular fluorometer, taking advantage of the fluorescence signal developed by the bound nucleotide analogue (*23*). The samples were irradiated with a 150-W mercury−xenon arc lamp at 410 nm excitation wavelength. The emission signal was selected with an OG515 cutoff filter (Ealing Electro-Optics, Holliston, MA). The composition of the reaction mixture is given in the legend for Figure 6.

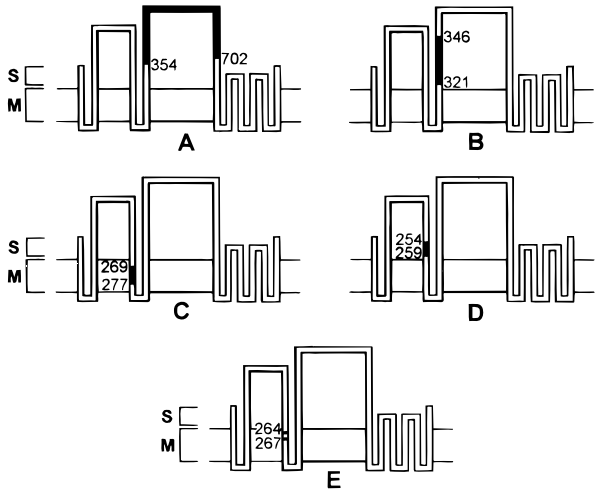

FIGURE 1: Diagrams of various chimeric mutations. The topology of the Ca^{2+}-ATPase sequence with respect to the membrane bilayer is represented according to MacLennan et al. (*29*). The two cytosolic loops are connected by stalk segments (S) to the transmembrane segments (M). The filled black lines indicate mutated amino acid-(s) within the Ca^{2+}-ATPase sequence. Scheme A was obtained by exchange between chicken SERCA1 cDNA (*12*) and chicken Na^+,K^+-ATPase α-subunits (*14*). Schemes B−E were obtained by additive mutations of chicken SERCA1 cDNA (*12*). See Materials and Methods for details.

Table 1: Site-Directed Mutations within the S3 Stalk Segment (Scheme D in Figure 1) of the Ca^{2+}-ATPase[a]

	sequence no.					
	254	255	256	257	258	259
WT Ca^{2+}-ATPase	Asp	Glu	Phe*	Gly	Glu	Gln
Mut 254,255	Glu*	His*				
Mut 254−257	Glu*	His*		Ile*		
Mut 254−258	Glu*	His*		Ile*	His*	
Mut 254−259	Glu*	His*		Ile*	His*	Leu*
Mut 256			Val			

[a] Additive mutations of two, three, four, and five amino acids of the Ca^{2+}-ATPase were made to the corresponding residues of the Na^+,K^+-ATPase (noted with *). Phe 256 is the only amino acid naturally conserved in both ATPases. For this reason, Phe256 was replaced with Val through a single-site-directed mutation.

RESULTS

Description of Mutants. The Ca^{2+}-ATPase segments that were subjected to mutations are indicated by the schemes shown in Figure 1. Unless otherwise stated, the mutations consisted of chimeric changes of Ca^{2+}-ATPase amino acids to the corresponding residues of the Na^+,K^+-ATPase.

Scheme A (Figure 1) shows a chimeric exchange of the large cytosolic loop of the Ca^{2+}-ATPase with the corresponding loop of the Na^+,K^+-ATPase (*8*). Scheme B shows an additive mutation of five amino acids to yield a chimeric segment of 26 amino acids in the S4 stalk segment, considering identical and conservative homologies in the native sequences (*24*). Scheme C shows a chimeric additive mutation of nine amino acids in the M3 transmembrane segment (*11*). Scheme D shows a six amino acid segment in the S3 stalk that was subjected to single and additive mutations. Since the D segment was subjected to detailed analysis, its specific mutations are listed in Table 1 above their replacements, which are marked with an asterisk (*) to indicate their correspondence to the Na^+,K^+-ATPase. Note

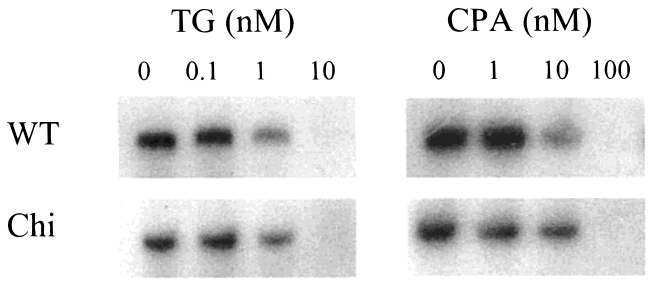

FIGURE 2: Effects of TG and CPA on phosphorylation of WT ATPase and chimera A by ATP. Phosphorylation was obtained as described in Materials and Methods. The concentrations of TG and CPA are given in nanomolar units.

that Phe256 is naturally conserved in both ATPases. Phe256 was then changed to Val since it was found that this single mutation occurs spontaneously in cell lines developing resistance to TG (*25*). Scheme E shows the location of two amino acids within the M3 segment (very close to the S3 segment) that were mutated to their Na^+,K^+-ATPase counterparts.

Expression of the mutants in COS-1 cells occurred at levels comparable to those of WT ATPase. At any rate, the expression levels were determined by Western blotting, and the resulting densitometric values were used to compare functional parameters of various preparations with reference to WT ATPase.

Sensitivities of Cytosolic Loop and S4 and M3 Chimeras to TG and CPA. Chimeric exchange of the large cytosolic loop (scheme A in Figure 1) produces strong inhibition of ATPase turnover but allows formation of phosphorylated enzyme intermediate by utilization of ATP. It was previously reported that, in analogy to the WT ATPase, phosphorylation of chimera A is strictly Ca^{2+} dependent and is still inhibited by TG (*8*−*10*). In our experiments, we titrated carefully the inhibition of the phosphorylation reaction by TG and CPA and found that the large chimera retains approximately the same sensitivity as observed with WT ATPase (Figure 2). These experiments suggest that the large cytosolic loop of the SERCA ATPase contributes relatively little to the binding affinity of the ATPase for TG and CPA.

Contrary to the large cytosolic loop chimera (A in Figure 1), neither a 26 amino acid chimera in transmembrane segment S4 (B in Figure 1) nor a nine amino acid chimera in transmembrane segment M3 (C in Figure 1) produce major interference with the Ca^{2+}-ATPase turnover. In fact, chimeras B and C retain 40% and 70% activity, respectively, when compared with the WT Ca^{2+}-ATPase (*11*). ATPase activity of both WT and chimeric enzymes proceed at constant rates when inhibition by accumulated Ca^{2+} is prevented by the addition of a Ca^{2+} ionophore.

With regard to sensitivity to TG or CPA, we found that no change was produced by the large chimeric replacement in the S4 transmembrane segment (B in Figure 1). Introduction of chimeric homology in the M3 transmembrane segment (C in Figure 1) produced only a slight reduction of sensitivity to both TG and CPA (Figure 3), as indicated by a 2−3-fold increase of the apparent K_i for either inhibitor (Table 2).

Sensitivities of S3 Stalk Segment Mutants to TG and CPA. All S3 stalk fragment mutants (scheme D in Figure 1) listed in Table 1 retained ATPase activity at levels that are

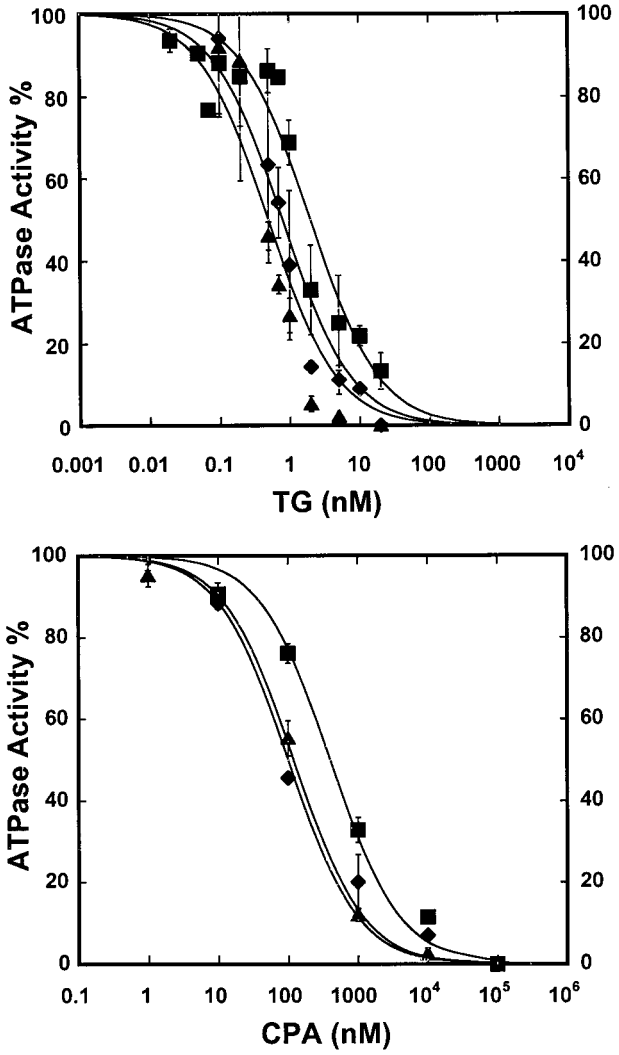

FIGURE 3: Inhibitory concentrations of TG and CPA on Ca^{2+}-ATPase activity of WT ATPase (▲) and mutated enzyme containing a 26-amino acid Na^+,K^+-ATPase homology in S4 as indicated in scheme B (♦) or a nine amino acid homology in M3 as indicated in scheme C (■). Ca^{2+}-dependent ATPase activity was measured as described in Materials and Methods. The experimental points were fitted assuming binding of a single inhibitory molecule per ATPase and using the K_i values listed in Table 2.

comparable to those of the wild-type enzyme. The only exceptions are the 254−258 and the 254−259 mutants that exhibited an approximately 50% reduction. We then could measure conveniently the concentration dependence of their inhibition by TG or CPA.

The 254−259, 254−258, and 254−257 mutants (corresponding to six, five, and four amino acid chimeric exchanges within the segment indicated in scheme D of Figure 1; see also Table 1) manifest a substantial reduction in sensitivity to both TG and CPA when compared to WT ATPase. The inhibition curves shown in Figure 4 and the apparent K_i values listed in Table 2 suggest that the reduction of sensitivity is greater for CPA than for TG. Furthermore, the four amino acid homology of mutant 254−257 is already sufficient to produce the maximal effect on sensitivity to CPA, while the effect on sensitivity to TG is gradually increased as the homology is raised from four to six amino acids.

The three amino acid homology mutation (254−255 in S3, within scheme D of Figure 1) decreases the ATPase

Table 2: Apparent K_i Values for Ca^{2+}-ATPase Inhibition by TG and CPA[a]

	TG		CPA	
sample	K_i	K_{iWT}/K_{iTG}	K_i	K_{iWT}/K_{iCPA}
WT Ca^{2+}-ATPase	0.5		120	
Chim S4 (B)	0.8	1.6	400	3.3
Chim M3 (C)	2.0	4.0	100	0.8
Mut 254, 255 (D)	1.1	2.2	400	3.3
Mut 254−257 (D)	6.0	12.0	30 000	250.0
Mut 254−258 (D)	10.0	20.0	30 000	250.0
Mut 254−259 (D)	50.0	100.0	30 000	250.0
Mut 256 (D)	20.0	40.0	350	2.9
Mut 264,267 (E)	1.0	2.0	200	1.7

[a] The values for WT Ca^{2+}-ATPase and various mutants were derived from the experiments shown in Figures 3−5. The letters in parentheses refer to the schemes in Figure 1. Note that the values listed in the table correspond to the apparent inhibitory constant. They are related to but do not correspond to dissociation constants (see Discussion). For a description of the mutants, see Table 1.

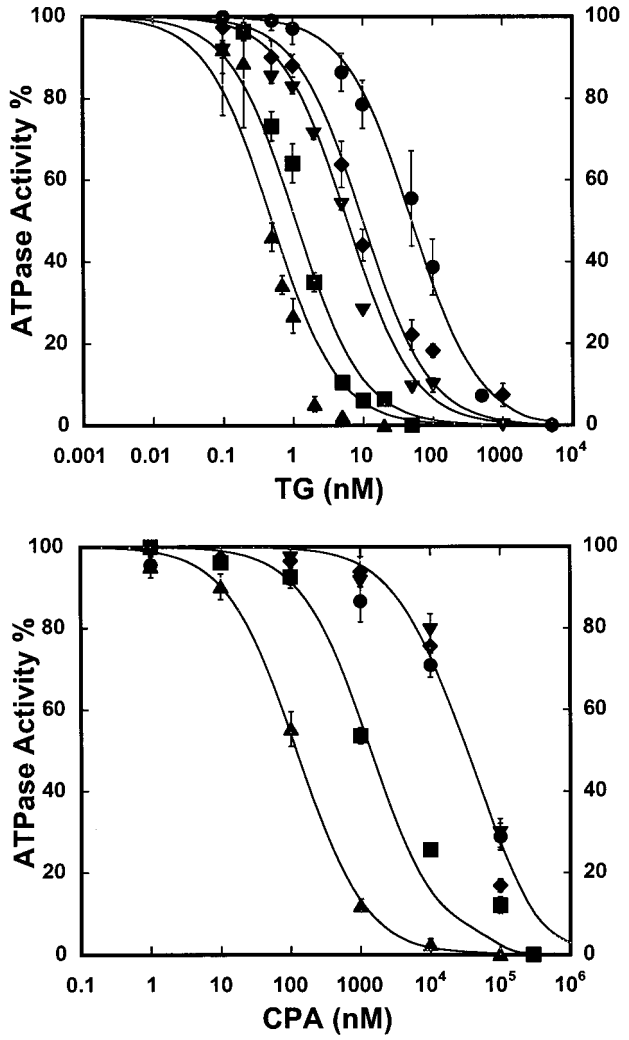

FIGURE 4: Inhibitory concentrations of TG and CPA on the Ca^{2+}-ATPase activity of WT ATPase (▲) and mutants 254,255 (■), 254−257 (▼), 254−258 (♦), and 254−259 (●) in S3 as indicated in scheme D. Ca^{2+}-dependent ATPase was measured as described in Materials and Methods. The experimental points were fitted assuming binding of a single inhibitory molecule per ATPase and assuming the K_i values listed in Table 2.

sensitivity to CPA by 1 order of magnitude, while the effect on the sensitivity to TG appears to be much lower (Figure 4 and Table 2).

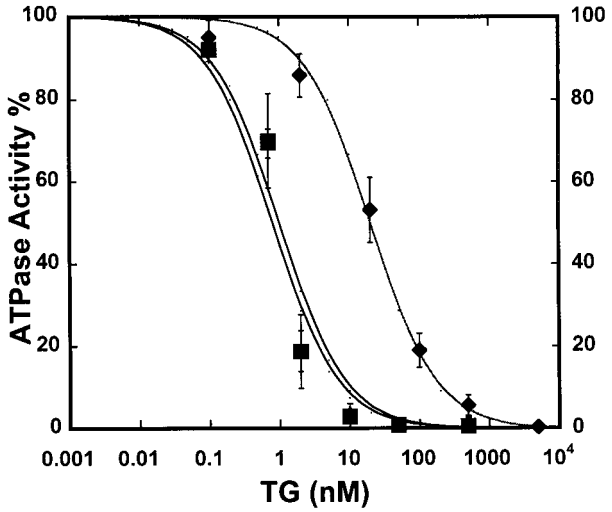

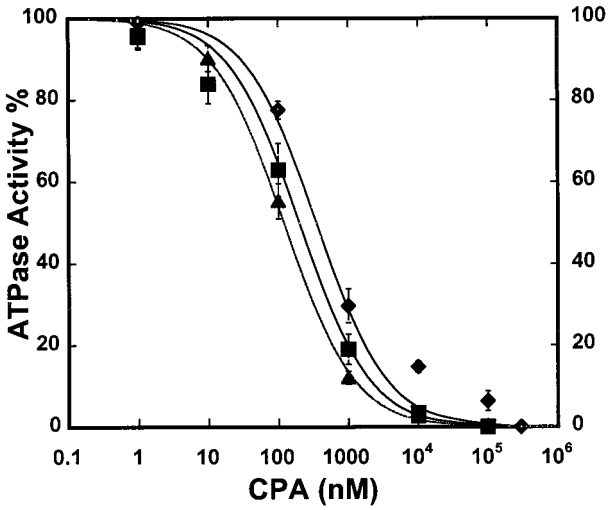

FIGURE 5: Inhibitory concentrations of TG and CPA on the Ca^{2+}-ATPase activity of WT ATPase (▲), mutant 264,267 in M3 as shown in scheme E (■), and the single mutant Phe256Val in S3 within the D segment (♦). Ca^{2+}-dependent ATPase was measured as described in Materials and Methods. The experimental points were fitted assuming binding of a single inhibitory molecule per ATPase and using the K_i values listed in Table 2.

It is of interest that single mutation of Phe256 (which is naturally conserved in both Ca^{2+} and Na^+,K^+-ATPases) to Val produces a marked reduction of the ATPase sensitivity to TG while having very little effect on the ATPase sensitivity to CPA (Figure 5 and Table 2). It is also interesting that the sensitivity of the S3 segment to mutations is quite localized within the S3 segment (scheme D in Figure 1). In fact, mutation of two (scheme E in Figure 1) or nine (scheme C in Figure 1) amino acids in the neighboring M3 segment has no significant effect on the concentration dependence of ATPase inhibition by either TG or PCA (Figures 3 and 5).

Effects of TG and CPA on the Displacement of TNP-ATP by ATP. The mutational analysis reported above suggests significant overlap of the TG and CPA binding domains within the S3 stalk segment of the ATPase. Since specific binding of TG and CPA is very difficult to measure directly, we attempted to obtain indirect evidence of mutual exclusion of the two inhibitors at the specific inhibitory site. To test the possibility of binding domain overlap, we then studied the effects of TG and PCA on the ability of ATP to displace

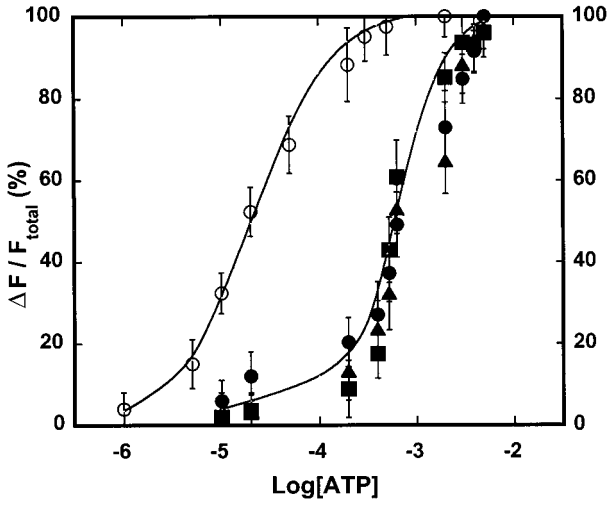

FIGURE 6: Displacement of bound TNP-ATP by ATP in the absence (○) and in the presence of TG (▲), CPA (●), or TG plus CPA (■). TNP-ATP binding to the SR ATPase was measured by fluorometry as explained in Materials and Methods. The reaction medium contained 20 mM MOPS, pH 7.0, 80 mM KCl, 5 mM $MgCl_2$, 0.2 mM EGTA, 0.2 mg of SR protein/mL, and 2 μM TNP-ATP. When indicated, 1 μM TG (▲), 1 μM CPA (●), or 1 μM TG and 1 μM CPA (■) were added to the medium. Displacement of bound TNP-ATP was assessed by monitoring the reduction of fluorescence following incremental additions of ATP. In these experiments, rabbit skeletal muscle SR vesicles were used as a source of wild-type Ca^{2+}-ATPase. Note that 0.2 mg of SR protein/mL corresponds approximately to 1 μM enzyme, which is therefore stoichiometrically equivalent to the concentrations of inhibitor used in the experiment.

the substrate analogue TNP-ATP from the nucleotide binding site (*26, 27*). In these experiments, we used SR vesicles obtained from rabbit skeletal muscle since their high content of wild-type Ca^{2+}-ATPase is well suited to spectroscopic measurements. In fact, bound TNP-ATP yields a very convenient fluorescence signal when bound to the Ca^{2+}-ATPase (*23*).

We found that ATP, in the micromolar range, displaces completely TNP-ATP from the nucleotide binding site. On the other hand, in the presence of TG or CPA producing total ATPase inhibition, the ATP concentration required for displacement of TNP-ATP is raised to the millimolar range, consistent with reduction of the ATPase affinity for ATP. It is of interest that, when the two inhibitors are added together, no additional increase of the ATP concentration required for TNP-ATP displacement is observed (Figure 6), suggesting that saturation of the effector site by one inhibitor prevents an effect by the alternate inhibitor. It should be pointed out that in these experiments the two inhibitors were used at micromolar concentrations in order to match the ATPase stoichiometry that was required by the measurements. The effects observed with ATPase and inhibitors matching stoichiometries imply that very low concentrations of either inhibitor remained free (nonbound) in the reaction mixture.

DISCUSSION

TG and CPA are two highly specific Ca^{2+}-ATPase inhibitors used extensively in experimental studies of intracellular Ca^{2+} signaling [see Inesi and Sagara (*28*) for a review]. The experiments reported here deal with the localization of the inhibitors' binding domains within the ATPase molecular structure. For this purpose, we consider the two-dimensional model proposed by MacLennan et al. (*29*) for the topology of the ATPase sequence. The model includes 10 membrane spanning (M) segments and two extramembranous loops, one of which is much larger that the other (Figure 1). In the folded structure of the protein, the two extramembranous loops form a cytosolic globular head connected through stalk segments (S) to the transmembrane segments (M). Several lines of evidence indicate that the ATP binding domain and the catalytic site reside within the cytosolic globular head of the ATPase, while the calcium binding domain resides within the transmembrane region [see Inesi et al. (*30*) and MacLennan et al. (*31*) for representative reviews].

Prior to this paper, most of the work on the ATPase inhibitory domain was aimed at localization of the TG binding site. Spectroscopic studies showed that TG, due to its strong hydrophobic character, partitions almost exclusively within or near the membrane phase of sarcoplasmic reticulum vesicles (*37*). On the other hand, mutational studies suggested that chimeric replacement of the entire M3−S3 segment increases the TG concentration required for ATPase inhibition (*10*). It was later found that it is actually the S3 stalk segment to play a most important role in determining the ATPase affinity for TG (*11*). We now find that the same S3 stalk segment is also involved in determining the ATPase affinity for CPA, as indicated by the effects of mutations. Inspection of Figure 4 and Table 2 suggests that mutational effects on the CPA apparent K_i are greater than those on the TG apparent K_i. The observed values, however, are apparent since we can only plot total rather than free inhibitor concentrations. This distinction is particularly important for TG, which is effective at concentrations seemingly equal to the WT ATPase stoichiometry (*3*). Therefore, the concentrations of free TG in the WT ATPase inhibition curves are certainly much lower than shown in the figures, and the displacement of the actual dissociation constants are likely to be much greater than indicated in Table 2. It should be understood that observed inhibitory constants are related to but in principle not identical to dissociation constants.

An interesting feature of the data shown in Figures 4 and 5 as well as in Table 2 is that various mutations affect differently the apparent TG K_i and the apparent CPA K_i. For instance, it takes additive mutations of 254 up to 259 to obtain incremental displacements of the TG concentration curve, while the maximal effect on the CPA concentration curve is obtained with the 254−257 mutation, and no additional effect is obtained with the 254−258 or 254−259 mutations (Figure 4). Furthermore, the Phe256→Val single mutation is effective on the TG concentration curve but not on the CPA concentration curve (Figure 5). The Phe256 residue is particularly important since spontaneous mutations of this residue to Leu, Ser, or Val were found in three cell lines following development of resistance to TG (*25, 33*). In fact, Phe256 is the only residue found to undergo spontaneous mutations as a consequence of selective pressure with TG.

Another important aspect of our experiments is that ATPase inhibition is still observed in all mutants as long as sufficient concentrations of inhibitors are used. Therefore, the mechanism of inhibition is not interfered with by our mutations. Rather, the effects of site directed and spontaneous

mutations indicate that the S3 stalk segment plays a role in the ATPase binding affinity for the inhibitors. It is likely that binding occurs by equilibration of inhibitor partitioned in the membrane lipids with a membrane interphase domain where interaction with S3 residues (and possibly others) provides specificity.

The overall analysis of our mutational experiments suggests that the TG and PCA binding domains overlap at the level of the S3 stalk segment. We then attempted to obtain independent evidence for such an overlap by studying the displacement of bound TNP-ATP by ATP. It was previously reported (*26*, *27*) that both TG and CPA increase the ATP concentration required to displace bound TNP-ATP from the ATPase. In our experiments, we found that the effects of TG and CPA are identical, and no additive effect is observed when both inhibitors are present at saturating concentrations (Figure 6). This suggests that the same reduction of the ATPase affinity for ATP is produced by occupancy of a single inhibitory domain by either TG or CPA.

Finally, an interesting question is how occupancy of an inhibitory site near the S3 stalk segment can influence the relatively distant nucleotide binding and catalytic domains. We consider, in this regard, that the coupling mechanism of ATP utilization and Ca^{2+} transport is based on a long-range intramolecular linkage (*34*) whereby phosphorylation of a catalytic aspartyl residue in the cytosolic region of the ATPase produces destabilization of calcium bound in the transmembrane region. In this mechanism, the clustered stalk segments provide a direct and functionally relevant connection between the aspartyl residue undergoing phosphorylation and the calcium binding domain. It is possible that inhibitory perturbations of the S3 stalk segment are transmitted through this long-range linkage to the nucleotide binding and catalytic domain. An interesting example of this effect is our previous finding that single mutation of Phe256 to Arg produces complete ATPase inhibition, while mutations of the same residue to Ala, Glu, Gly, Leu, Ser, Ile, Thr, Tyr, or Val do not (*25*). This inhibitory effect is most likely related to charge interaction (or repulsion) between the Arg introduced at position 256 and other neighboring charged residues. It is possible that a similar inhibitory perturbation is produced by occupancy of TG and CPA binding domains in the S3 stalk segment.

ACKNOWLEDGMENT

Figures and manuscript were edited by Jerry Domanico.

REFERENCES

1. Rasmussen, U., Christensen, S. B., and Sandberg, F. (1978) *Acta Pharm. Suec. 15*, 133.
2. Cole, R. J. (1984) in *Mycotoxins-Production, Isolation, Separation and Purification* (Betina, V., Ed.) Elsevier, Amsterdam.
3. Sagara, Y., and Inesi, G. (1991) *J. Biol. Chem. 266*, 13503.
4. Lytton, J., Westlin, M., and Hanley, M. R. (1991) *J. Biol. Chem. 266*, 17067.
5. Goeger, D. E., Riley, R. T., Dorner, J. W., and Cole, R. J. (1988) *Biochem. Pharmacol. 37*, 978.
6. Seidler, N. W., Jona, I., Vegh, M., and Martonosi, A. (1989) *J. Biol. Chem. 264*, 17816.
7. Soler, F., Plenge-Tellechea, F., Fortea, I., and Fernandez-Belda, F. (1998) *Biochemistry 37*, 4266.
8. Sumbilla, C., Lu, L., Inesi, G., Ishii, T., Takeyasu, K., Fang, Y., and Fambrough, D. M. (1993) *J. Biol. Chem. 268*, 21185.
9. Norregaard, A., Vilsen, B., and Andersen, J. P. (1993) *FEBS Lett. 336*, 248.
10. Norregaard, A., Vilsen, B., and Andersen, J. P. (1994) *J. Biol. Chem. 269*, 26598.
11. Zhong, L., and Inesi, G. (1998) *J. Biol. Chem. 273*, 12994.
12. Karin, N. J., Kaprielian, Z., and Fambrough, D. M. (1989) *Mol. Cell. Biol. 9*, 1978.
13. Ho, S. N., Hunt, H. D., Horton, R. M., Pullen, J. K., and Pease, L. R. (1989) *Gene 77*, 51.
14. Takeyasu, K., Tamkun, M. M., Renaud, K. J., and Fambrough, D. M. (1988) *J. Biol. Chem. 263* (9), 4347.
15. Takebe, Y., Seiki, M., Fujisawa, J. I., Hoy, P., Yokota, K., Arai, K. I., Yoshida, M., and Arai, N. (1988) *Mol. Cell. Biol. 8*, 466.
16. Lopata, M. A., Cleveland, D. W., and Sollner-Webb, B. (1984) *Nucleic Acids Res. 12*, 5707.
17. Strock, C., Cavagna, M., Peiffer, W., Sumbilla, C., Lewis, D., and Inesi, G. (1998) *J. Biol. Chem. 273*, 15104.
18. Lebovitz, R. M., Takeyasu, K., and Fambrough, D. M. (1989) *EMBO J. 8*, 193.
19. Eletr, S., and Inesi, G. (1972) *Biochim. Biophys. Acta 282*, 174.
20. Lowry, O. H., Roseborough, N. J., Farr, A. L., and Randall, R. J. (1951) *J. Biol. Chem. 193*, 265.
21. Lanzetta, P. A., Alvarez, L. J., Reinsch, P. S., and Candia, O. A. (1979) *Anal. Biochem. 100*, 95.
22. Weber, K., and Osborn, M. (1969) *J. Biol. Chem. 244*, 4406.
23. Watanabe, T., and Inesi, G. (1982) *J. Biol. Chem. 257*, 11510.
24. Garnett, C., Sumbilla, C., Fernandez Belda, F., Chen, L., and Inesi, G. (1996) *Biochemistry 35*, 11019.
25. Yu, M., Lin, J., Khadeer, M., Yeh, Y., Inesi, G., and Hussain, A. (1999) *Arch. Biochem. Biophys. 362*, 225.
26. DeJesus, F., Girardet, J.-L., and Dupont, Y. (1993) *FEBS Lett. 332*, 229.
27. Plenge-Tellechea, F., Soler, F., and Fernandez-Belda, F. (1997) *J. Biol. Chem. 272*, 2794.
28. Inesi, G., and Sagara, Y. (1994) *J. Membr. Biol. 141*, 1.
29. MacLennan, D. H., Brandl, C. J., Korczak, B., and Green, N. M. (1985) *Nature 316*, 696.
30. Inesi, G., Sumbilla, C., and Kirtley, M. E. (1990) *Physiol. Rev. 70*, 749.
31. MacLennan, D. H., Rice, W. J., and Green, N. M. (1997) *J. Biol. Chem. 272*, 28815.
32. Hua, S., Malak, H., Lakowicz, J. R., and Inesi, G. (1995) *Biochemistry 34*, 5137.
33. Yu, M., Zhong, L., Rishi, A. K., Khadeer, M., Inesi, G., and Hussain, A. (1998) *J. Biol. Chem. 273*, 3542.
34. Inesi, G., Lewis, D., Nikic, D., and Kirtley, M. E. (1992) in *Advances in Enzymology* (Meister, A., Ed.) pp 185−215, John Wiley and Sons, New York.

BI991523Q